

Concentration dependence of energy transfer between Eu^{3+} ions occupying two symmetry sites in Lu_2O_3

This article has been downloaded from IOPscience. Please scroll down to see the full text article.

2002 J. Phys.: Condens. Matter 14 5637

(<http://iopscience.iop.org/0953-8984/14/22/315>)

View [the table of contents for this issue](#), or go to the [journal homepage](#) for more

Download details:

IP Address: 171.66.16.104

The article was downloaded on 18/05/2010 at 06:47

Please note that [terms and conditions apply](#).

Concentration dependence of energy transfer between Eu^{3+} ions occupying two symmetry sites in Lu_2O_3

E Zych¹

Faculty of Chemistry, University of Wrocław, 14 F Joliot-Curie Street, 50-383 Wrocław, Poland

E-mail: zych@wchuwr.chem.uni.wroc.pl

Received 14 December 2001, in final form 17 April 2002

Published 23 May 2002

Online at stacks.iop.org/JPhysCM/14/5637

Abstract

A series of Lu_2O_3 samples doped with Eu was prepared in the form of sintered tablets. The activator concentration was 0.2, 1, 3, 5, 7 and 10% with respect to Lu. Emission spectra excited with light of various energies were taken at liquid nitrogen and room temperature. Excitation spectra of characteristic Eu emission lines for two different symmetry sites in Lu_2O_3 (C_2 and S_6) were also recorded. It was shown that Eu ions located in the two different symmetry sites possess characteristic excitation spectra in the regions both of the ${}^7F_0 \rightarrow {}^5D_1$ absorption and of the charge transfer transitions. In both cases the levels of the $\text{Eu}(S_6)$ ions were located above those of the $\text{Eu}(C_2)$. In both emission and excitation spectra an energy transfer from Eu ions occupying the centrosymmetric S_6 site in Lu_2O_3 to Eu ions in the noncentrosymmetric C_2 site was observed. Some indications were found that an opposite back-transfer (from Eu in C_2 to Eu in the S_6 site) also occurs. Lower temperature significantly reduces the rate of the $\text{Eu}(S_6) \rightarrow \text{Eu}(C_2)$ transfer. Decay kinetics indicated that even at room temperature the $\text{Eu}(S_6)$ emission could be further reduced if the dopant content was higher than 10%. Both at room and liquid nitrogen temperatures the decay kinetics of the $\text{Eu}(C_2)$ emissions are characterized by the time constants of about 1.0 ms for all concentrations, indicating that up to 10% of the dopant content no concentration or thermal quenching takes place. The liquid nitrogen $\text{Eu}(S_6)$ luminescence is characterized by a time constant of about 7 ms for the 0.2% specimen. At room temperature this value decreases to 5.6 ms.

1. Introduction

Lutetium oxide has recently attracted rising interest from the scientific community [1–8]. While its price is still rather high, it dropped drastically to a reasonable level during the last decade. The interest in Lu_2O_3 has various reasons but it seems that the most important one is

¹ <http://www.chem.uni.wroc.pl/personal/zych.htm>.

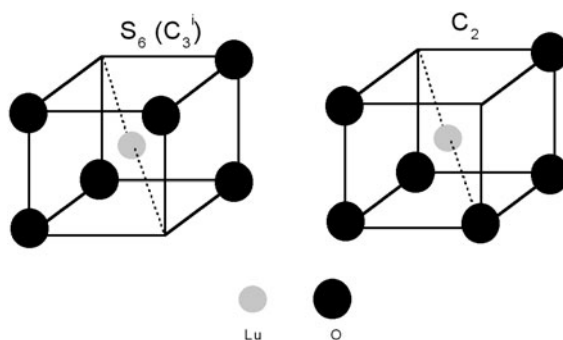


Figure 1. Depiction of the two Lu^{3+} symmetry sites in Lu_2O_3 .

Table 1. Characteristic inter-ionic distances in Lu_2O_3 .

Lu ion	O ion	Inter-atomic distance (Å)	Site symmetry
$8 \times \text{Lu}(1)$	$6 \times \text{O}$	2.247	$S_6 (C_3^i)$
$24 \times \text{Lu}(2)$	$2 \times \text{O}$	2.183	C_2
	$2 \times \text{O}$	2.239	
	$2 \times \text{O}$	2.282	
$\text{Lu}(1)\text{--Lu}(1)$		5.195	
$\text{Lu}(2)\text{--Lu}(2)$		3.460	
$\text{Lu}(1)\text{--Lu}(2)$		3.433	

that the material shows an exceptionally high absorption coefficient for ionizing radiation. The stopping power for x-rays and gamma rays is very high mostly due to the very high density of the oxide (9.42 g cm^{-3}). Additionally, since Lu has a very high Z -number (71), the energy of an incoming gamma- or x-ray particle can be preferentially stopped at a single position in the material instead of, due to Compton scattering, a few spatially separated positions [9]. Such a situation is very suitable since it allows achievement of higher-resolution images in medical diagnosis [9, 10]. Furthermore, lutetia is practically not affected by the ambient atmosphere components, which is, obviously, a very desirable property.

Lu_2O_3 represents the rare-earth sesquioxide C-type of structure, the same one as Y_2O_3 [11–14], a well known commercial phosphor when doped with Eu. The cubic unit cell is characterized by $a = 10.39 \text{ Å}$ and $Z = 16$. The structure offers two sites for the metal ion as depicted in figure 1. In each of them the Lu^{3+} ion is surrounded by six oxygen ions. 24 of the 32 Lu ions residing in the unit cell are characterized by C_2 site symmetry (noncentrosymmetric, $\text{Lu}(C_2)$), while the other eight Lu ions possess $S_6 (C_3^i)$ site symmetry (centrosymmetric, $\text{Lu}(S_6)$). The Lu ions form two types of layer in the lutetia crystal lattice. One of them consists of $\text{Lu}(C_2)$ ions exclusively, while the other contains equal numbers of $\text{Lu}(C_2)$ and $\text{Lu}(S_6)$ ions [11]. The inter-ionic distances important for spectroscopic considerations are listed in table 1. As we can see the shortest distance between the metal ions is in the case of the $\text{Lu}(S_6)\text{--Lu}(C_2)$ pair. Therefore, the nearby located ions occupying these sites can be expected to interact most severely.

The structure of lutetium oxide has important implications for its spectroscopic properties when activated with luminescent ions. First of all, it is not obvious that the dopant will enter the two different host lattice sites with equal probabilities. It is possible that the Eu ion will preferentially occupy one of the available symmetry sites, especially since the Eu^{3+} ion is 10% larger than the substituted Lu^{3+} ion (0.947 versus 0.861 Å) [15]. Obviously, the

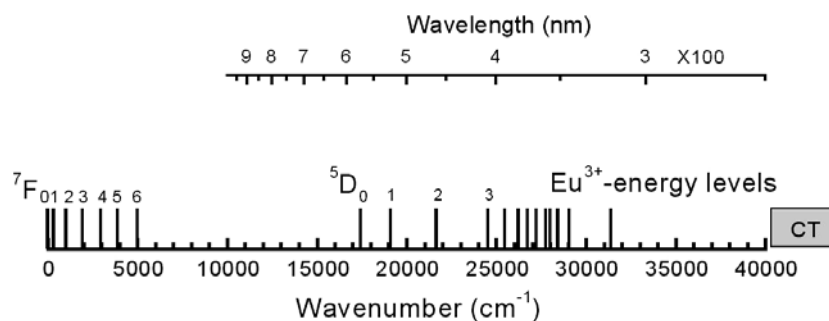


Figure 2. The structure of the Eu^{3+} free-ion energy levels.

different symmetries of the Eu environments must result in different spectroscopic properties of the $\text{Eu}(\text{C}_2)$ and $\text{Eu}(\text{S}_6)$ ions. In general terms the intraconfigurational f–f electric dipole transitions are totally forbidden for centrosymmetric sites since the levels have the same parity. In such a case only magnetic dipole transitions can occur. These are in general weaker than electric dipole transitions. For noncentrosymmetric sites the crystal-field interaction introduces an opposite-parity part to the potential energy of the crystal levels, which makes the electric dipole transitions also possible in emission and absorption as well [16].

In the case of our title phosphor, $\text{Lu}_2\text{O}_3:\text{Eu}$, for Eu ions located in the S_6 (centrosymmetric) sites only the f–f magnetic dipole transitions can be expected. This means that the initial and terminating levels must fulfill the condition $\Delta J = 0$ or 1 and $J = 0 \rightarrow J = 0$ transition is also totally forbidden [16, 17]. The situation differs significantly for the Eu ions occupying the C_2 site, for which the electric dipole transitions can also be observed. Thus, considering the electronic level structure of Eu^{3+} (see figure 2, [18]), for ions residing in the centre of inversion (S_6) we expect exclusively $7F_0 \rightarrow 5D_1$ transitions in absorption/excitation spectra and $5D_0 \rightarrow 7F_1$ (and eventually traces of $5D_1 \rightarrow 7F_0$) in emission spectra. For the Eu^{3+} ions occupying the C_2 site basically all the intraconfigurational f–f transitions can occur, which for emission means that mostly the $5D_0 \rightarrow 7F_j$ lines can be expected. Let us additionally note that the levels of $\text{Eu}(\text{S}_6)$ characterized by the quantum number $J = 1$ ($7F_1$, $5D_1$) can split in the centrosymmetric surrounding into two Stark components, one of which is doubly degenerated. In the case of $\text{Eu}(\text{C}_2)$ ions these levels split into three components [19–21]. Thus, for $\text{Eu}(\text{S}_6)$ we should expect two $7F_0 \rightarrow 5D_1$ lines in excitation and also two $5D_0 \rightarrow 7F_1$ lines in emission. Analogous transitions within $\text{Eu}(\text{C}_2)$ should produce three lines in appropriate spectra.

However, we should remember that the intraconfigurational transitions within the $4f^6$ levels of the Eu^{3+} ion are not the only ones possible. In oxides the $\text{Eu}^{3+}-\text{O}^{2-}$ charge-transfer (CT) state is located at relatively low energy [10]. The CT transition probabilities are not affected by the surrounding symmetry in the same way as the f–f transitions although, obviously, their positions can change. As we shall see this fact can be very useful to track energy-transfer processes between Eu^{3+} ions located in the various sites of the Lu_2O_3 host lattice.

From a practical point of view the presence of the S_6 site is not convenient, because the Eu^{3+} ions residing there can only produce much slower (due to the lower probability of the transitions [16, 22]) emission, and this also raises the probability of nonradiative relaxations, which would hamper the total emission efficiency. Thus we would prefer to tailor the phosphor in such a way that the emission would be basically due to Eu ions occupying the C_2 site, while the $\text{Eu}(\text{S}_6)$ luminescence would be strongly or even totally diminished. Defining such conditions was one of the goals of our work.

2. Materials and experiments

We prepared a series of samples of $\text{Lu}_2\text{O}_3:\text{Eu}$ containing 0.2, 1, 3, 5, 7 and 10 mol% of Eu with respect to Lu. The specimens were in the form of semitransparent tablets. The 10 mm diameter pellets were vacuum sintered at 1700 °C for 5 h following cold-pressing of appropriate powders under 9 tonnes of load. The powders were prepared combusting an appropriate mixture of $\text{Lu}(\text{NO}_3)_3 \cdot 5\text{H}_2\text{O}$ and $\text{Eu}(\text{NO}_3)_3 \cdot 6\text{H}_2\text{O}$ with glycine in a furnace preheated up to 650 °C. The blend was obtained by dissolving the nitrates and the glycine in water followed by drying at 140 °C for about 2–3 h. More details of the synthesis of the raw powders can be found in [6–8].

Luminescence and excitation spectra were recorded with an SPF 500 spectrofluorimeter equipped with a 300 W Xe lamp with a sapphire window and an Al-coated parabolic reflector. Both excitation and emission monochromators were of 0.25 m focal length and $f/4$ aperture. The emission monochromator was equipped with a 1200 line mm^{-1} ruled grating blazed at 500 nm, while the excitation monochromator used a 1200 line mm^{-1} holographic grating optimized for 250–300 nm. Excitation spectra were corrected for the excitation light intensity. Emission spectra were not corrected for the setup characteristic, and the sensitivity of the detection system (PMT grating) was highest in the range of 400–750 nm. The spectra were measured at liquid nitrogen or room temperature.

Emission kinetics were measured with a Tektronics 1000 TDS 380 oscilloscope using excimer laser (308 nm) as an excitation source. The emission lines were selected with a Jobin Yvon spectrophotometer. The measurements were performed at room and liquid nitrogen temperatures.

3. Results and discussion

In figure 3 we show emission spectra of the $\text{Lu}_2\text{O}_3:\text{Eu}$ specimens taken at liquid nitrogen temperature under 250 nm excitation. All spectra are very similar and contain almost the same features. Nevertheless, the ratio of some of the transition intensities, when related to the main line located at 611.4 nm, significantly and systematically decreases with Eu concentration. Below 580 nm we can see some relatively weak lines, which can be assigned to the radiative return from the $^5\text{D}_1$ (530–540 nm) and eventually $^5\text{D}_2$ (~502 nm) Eu^{3+} states. Their intensities when related to the strongest hypersensitive $^5\text{D}_0 \rightarrow ^7\text{F}_2$ line at 611.4 nm systematically decrease with Eu content. Lines located below 530 nm completely disappear for higher concentrations. Above 580 nm we can see a complex set of lines, which are known as the characteristic red luminescence of Eu^{3+} . As we discussed in the introduction the 580–605 nm region (see figure 2) of the spectrum may contain lines resulting both from the europium ions residing in the C_2 site and those in the S_6 site. Indeed, excitation spectra of selected lines confirmed the existence of europium in two different environments. In figure 4 we present the $^7\text{F}_0 \rightarrow ^5\text{D}_1$ and the CT regions of the excitation spectra of the 611.4 nm emission for $\text{Lu}_2\text{O}_3:\text{Eu}$ samples with varying Eu content, and the excitation spectrum of the 582.8 nm line for the most diluted (0.2%) specimen. For the latter sample, for which the possible Eu–Eu interaction should be negligible due to the low concentration, we clearly see that the excitation spectra of the 611.4 and 582.8 nm lines are different in both $^7\text{F}_0 \rightarrow ^5\text{D}_1$ and CT regions, which confirms that the two monitored emissions result from spectroscopically different europium ions. Hence, knowing the lutetia crystal structure we can attribute the 582.8 nm line to the $^5\text{D}_0 \rightarrow ^7\text{F}_1$ emission from the $\text{Eu}(\text{S}_6)$ ion, since the 611.4 nm line must necessary result from the $^5\text{D}_0 \rightarrow ^7\text{F}_2$ transition of the $\text{Eu}(\text{C}_2)$ ion, as it is the electric dipole luminescence. For the 582.8 nm emission ($\text{Eu}(\text{S}_6)$, $^5\text{D}_0 \rightarrow ^7\text{F}_1$) the characteristic for the CT absorption band peaks around 237 nm, while for the 611.4 nm emission ($\text{Eu}(\text{C}_2)$, $^5\text{D}_0 \rightarrow ^7\text{F}_2$) the band shifts toward lower energies and peaks

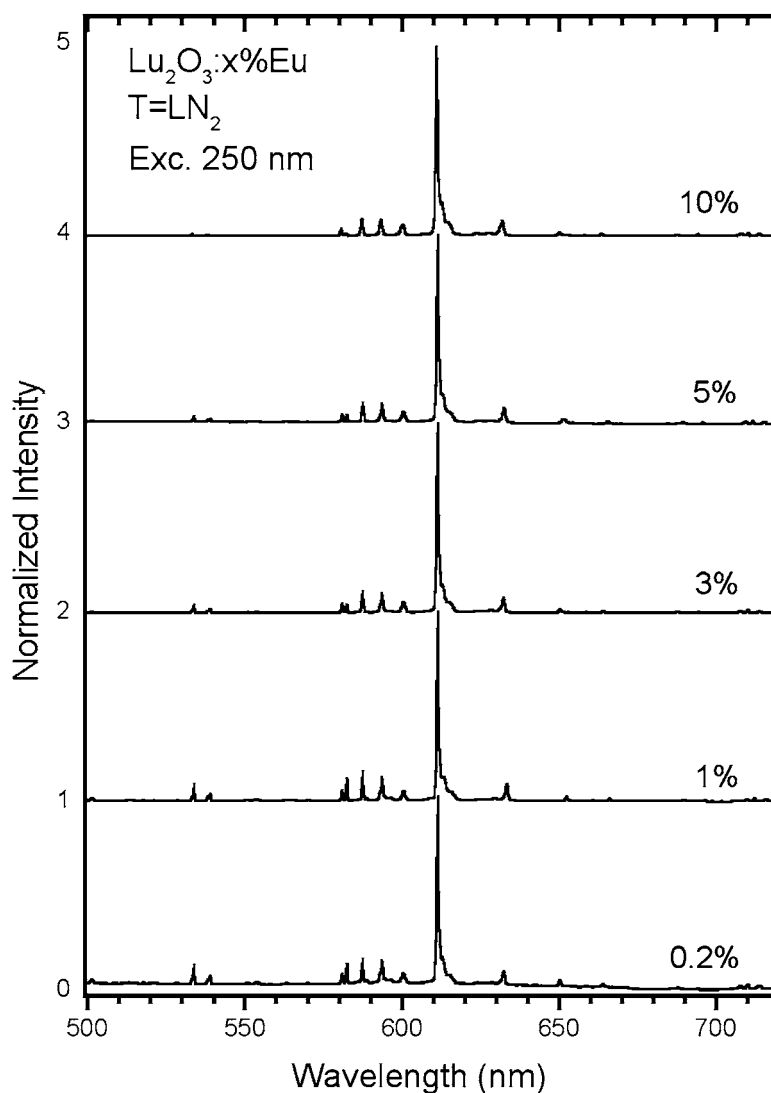


Figure 3. Concentration dependence of the liquid nitrogen temperature emission spectra of $\text{Lu}_2\text{O}_3:x\% \text{Eu}$ under 250 nm excitation.

around 247 nm. Thus from the excitation spectra of the diluted specimen presented in figure 4 we can conclude that the levels of the europium ions located in S_6 surrounding symmetry are characterized by higher energies than levels of the $\text{Eu}(C_2)$. This is true for both the $4f^6$ and the CT states. Figure 4 shows also that the excitation spectra of the 611.4 nm luminescence systematically change with rising dopant concentration. One of the observed effects is that both the $f-f$ lines and the CT bands broaden when the dopant content increases. Obviously, for the $f-f$ lines this effect is only subtle since the $4f$ levels are well shielded from the external environment's influence. However in the case of the CT transition the broadening is very profound and causes a shift of the peak position from 247 nm for the most diluted system up to about 275 nm for the 10% specimen. Such a behaviour can be attributed to an increasing

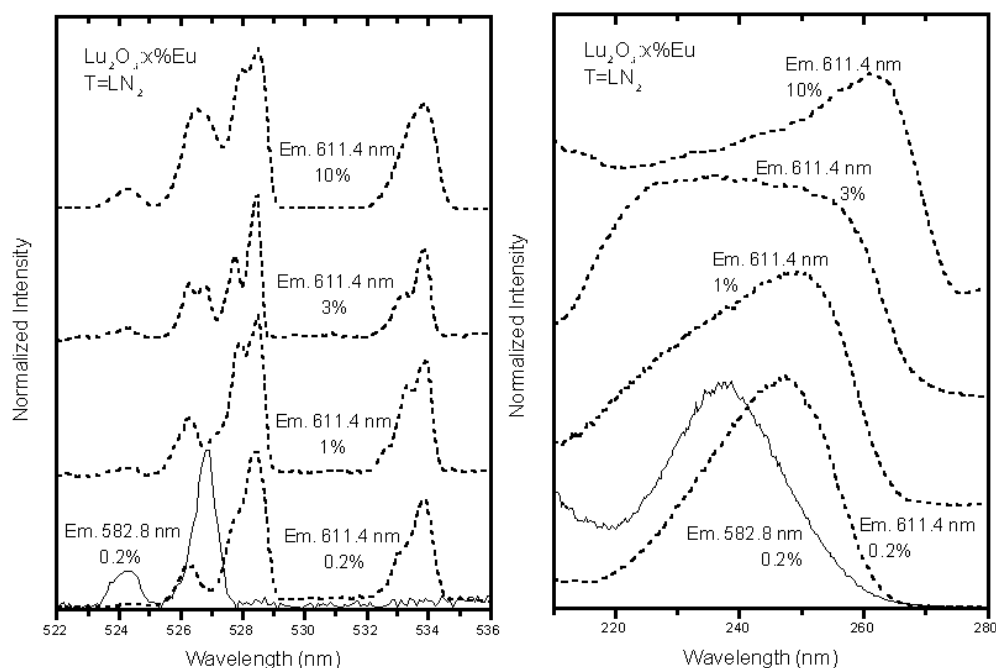


Figure 4. Excitation spectra of the 611.4 nm emission characteristic for the C_2 site and of the 582.8 nm luminescence characteristic for the S_6 site in the region of the ${}^7F_0 \rightarrow {}^5D_1$ (left) and CT absorption (right). Spectra taken at liquid nitrogen temperature.

interaction between the Eu ions due to the shortening of the mean inter-ionic distances. Another concentration effect clearly seen in both the ${}^5D_0 \rightarrow {}^7F_1$ and the CT excitation regions is the appearance of the excitation transitions characteristic for $Eu(S_6)$ ions in the excitation spectra of the $Eu(C_2)$ emission (611.4 nm) for higher activator contents. In the region of the CT band this results in increasing intensity around 230 nm while in the case of the ${}^5D_0 \rightarrow {}^7F_1$ transitions it results in systematically increasing intensity of the 524.2 and 526.8 nm lines (characteristic for the $Eu(S_6)$ absorption) in the excitation of the $Eu(C_2)$ 611.4 nm luminescence. Obviously, such behaviour clearly indicates the increasing rate of the energy transfer from the excited $Eu(S_6)$ to the nearby located $Eu(C_2)$ ions. From table 1 we see that the shortest possible distance is between the $Eu(C_2)$ and $Eu(S_6)$ ions, which makes the energy transfer between them most probable. Additionally, we have already noted that the f-f levels of the $Eu(S_6)$ ions are located above those of the $Eu(C_2)$ ions by about 55 cm^{-1} (at least for the ${}^5D_0 \rightarrow {}^7F_1$ region, see figure 4). In such a case the $Eu(C_2) \rightarrow Eu(S_6)$ energy transfer should be much less probable than the $Eu(S_6) \rightarrow Eu(C_2)$ one, although the former cannot be completely excluded as the relatively high temperature of the liquid nitrogen makes appropriate-energy phonons still available. Later we shall see that such a back-transfer does indeed take place. Nevertheless, in every case the $Eu(S_6) \rightarrow Eu(C_2)$ transfer should dominate and this we indeed observe.

The excitation spectra in the region of the ${}^7F_0 \rightarrow {}^5D_1$ absorption convince us also that for diluted specimens it should be possible to excite independently the characteristic emissions of the two crystallographically different europium ions. Indeed, as seen in figure 5, exciting the specimens with 524.2 nm (S_6) or 533.8 nm (C_2), we were able to reasonably separate the previously overlapping (see figure 3) emissions of $Eu(C_2)$ and $Eu(S_6)$. We should note, however, that it was not possible to record pure emission of either $Eu(C_2)$ or $Eu(S_6)$ ions.

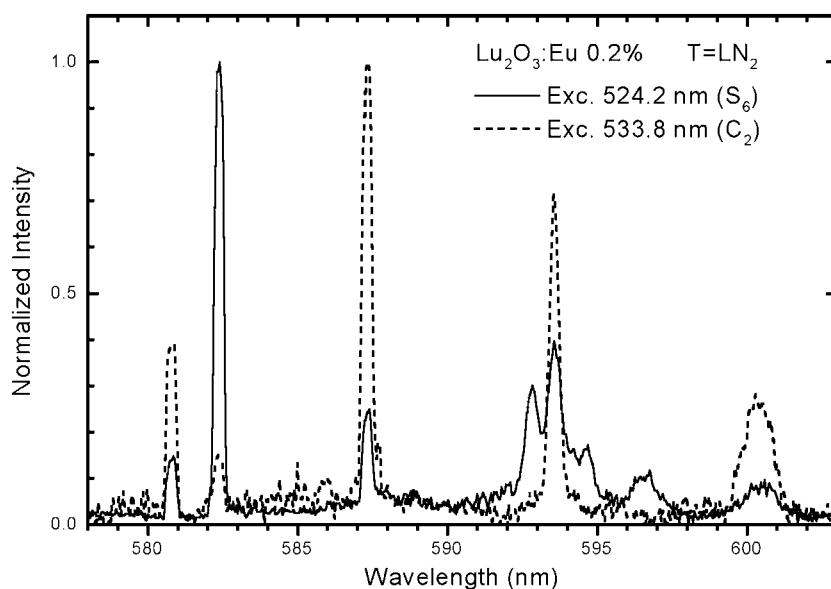


Figure 5. Emission spectra of $\text{Lu}_2\text{O}_3:0.2\%\text{Eu}$ under selective excitation of the $\text{Eu}(\text{S}_6)$ (solid curve) and $\text{Eu}(\text{C}_2)$ ions taken at liquid nitrogen temperature. Spectra taken with 0.05 nm resolution.

We observed the same exciting the materials into the $^5\text{D}_2$ (465 nm) or $^5\text{D}_3$ states (394 nm, see figure 2). These observations indicate the existence of energy transfer processes between europium ions occupying the two different sites. This, however, is slightly surprising for such a diluted sample (0.2%), for which the probability that the ions of activator will reside close enough to exchange energy should be small if the Eu ions do not have significant tendency to aggregate. The aggregation, on the other hand, cannot be excluded. Especially surprising is that we could not record pure emission of the $\text{Eu}(\text{C}_2)$. As we already noted, the energy levels of these ions are located slightly below the levels of the $\text{Eu}(\text{S}_6)$ (by some 55 cm^{-1} , see figure 4). In such a case the $\text{Eu}(\text{C}_2) \rightarrow \text{Eu}(\text{S}_6)$ energy transfer should be suppressed and the excitation into the $\text{Eu}(\text{C}_2)$ should result exclusively in this ion emission. Since this is not the case we can conclude that the energy difference between the $\text{Eu}(\text{C}_2)$ and $\text{Eu}(\text{S}_6)$ is small enough for the back-transfer $\text{Eu}(\text{C}_2) \rightarrow \text{Eu}(\text{S}_6)$ to be phonon mediated even at liquid nitrogen temperature. More definitive considerations cannot, however, be made without measurements at liquid helium temperature, at which such phonon-assisted transitions would be practically absent. From excitation spectra (figure 4) we know, however, that the most efficient, and increasing with concentration, is the $\text{Eu}(\text{S}_6) \rightarrow \text{Eu}(\text{C}_2)$ energy transfer.

The results presented in figures 4 and 5 allow us to construct a realistic, though not complete, energy diagram for the states $^7\text{F}_0$, $^7\text{F}_1$, $^5\text{D}_0$, and $^5\text{D}_1$ both for $\text{Eu}(\text{S}_6)$ and $\text{Eu}(\text{C}_2)$ and correlate their mutual positions. Such a scheme is given in figure 6. Clearly, both the $^5\text{D}_1$ and the emitting $^5\text{D}_0$ state of $\text{Eu}(\text{S}_6)$ are located noticeably higher than analogous level of $\text{Eu}(\text{C}_2)$. In table 2 we compare the observed energies of Eu^{3+} crystal levels in Lu_2O_3 with the results obtained by other authors [19–21] for $\text{Y}_2\text{O}_3:\text{Eu}$, a structural analogue of lutetia. The presented comparison proves that the energies of Eu^{3+} ion levels in both host lattices are very similar. The similarity allows us to estimate the lacking numbers in our diagram shown in figure 6. Assuming that the position of the lower component of the $^7\text{F}_1$ term of $\text{Eu}(\text{S}_6)$ in Lu_2O_3 is equal to that in Y_2O_3 (132 cm^{-1}) we can estimate the position of the $^5\text{D}_0$ state of $\text{Eu}(\text{S}_6)$ in

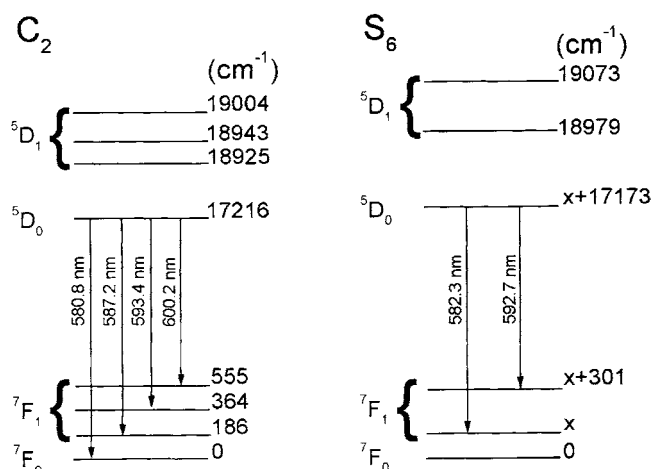


Figure 6. Schematic of energy levels of $\text{Eu}(\text{C}_2)$ and $\text{Eu}(\text{S}_6)$ for the lowest manifolds of the ^5D and ^7F terms in $\text{Lu}_2\text{O}_3:\text{Eu}$. x can be estimated to be $\sim 132 \text{ cm}^{-1}$ (see text).

Table 2. Energy of selected levels of Eu^{3+} in Lu_2O_3 and their comparison to the levels in Y_2O_3 . Results for the latter are taken from [17, 18], $x \sim 132 \text{ cm}^{-1}$, see text.

Symmetry site	Multiplet	Energy in Lu_2O_3 (cm^{-1})	Observed energy in Y_2O_3 (cm^{-1})	Calculated energy in Y_2O_3 (cm^{-1})
$\text{Eu}(\text{C}_2)$	$^7\text{F}_0$	0	0	-1
	$^7\text{F}_1$	186	199	199
		364	360	349
		555	543	555
	$^5\text{D}_0$	17 216	17 216	17 216
$^5\text{D}_1$	18 925	18 930	18 915	
	18 943	18 954	18 941	
	19 004	18 992	19 019	
$\text{Eu}(\text{S}_6)$	$^7\text{F}_0$	0	0	0
	$^7\text{F}_1$	x	132	132
		$x + 301$	432	432
	$^5\text{D}_0$	$x + 17 173$	17 302	—
	$^5\text{D}_1$	18 979	18 992	—
19 073		19 084	—	

lutetia. Such calculations give the energy of $17\,305 \text{ cm}^{-1}$ for the $^5\text{D}_0$ level of $\text{Eu}(\text{S}_6)$ ion in Lu_2O_3 . That locates the $^5\text{D}_0$ level of $\text{Eu}(\text{S}_6)$ 89 cm^{-1} above its analogue of $\text{Eu}(\text{C}_2)$. This is a very reasonable number comparing to the $86\text{--}87 \text{ cm}^{-1}$ in Y_2O_3 [19–21]. Until we have more reliable results of direct measurements of the value for $\text{Lu}_2\text{O}_3:\text{Eu}$ the numbers we find can certainly be treated as a reasonable estimation of the separation of the $^5\text{D}_0$ levels for $\text{Eu}(\text{C}_2)$ and $\text{Eu}(\text{S}_6)$ sites in this host. We can also note (see table 2) that the crystal field splitting of Eu^{3+} levels is slightly bigger in Lu_2O_3 than in Y_2O_3 , exactly as would be expected since Lu^{3+} is a smaller ion compared to Y^{3+} .

The $\text{Eu}(\text{C}_2) \rightarrow \text{Eu}(\text{S}_6)$ energy transfer can also be nicely observed in emission spectra. In figure 7 we show the concentration dependence of such spectra recorded at liquid nitrogen temperature when the materials are irradiated with 230 nm light. This light preferentially

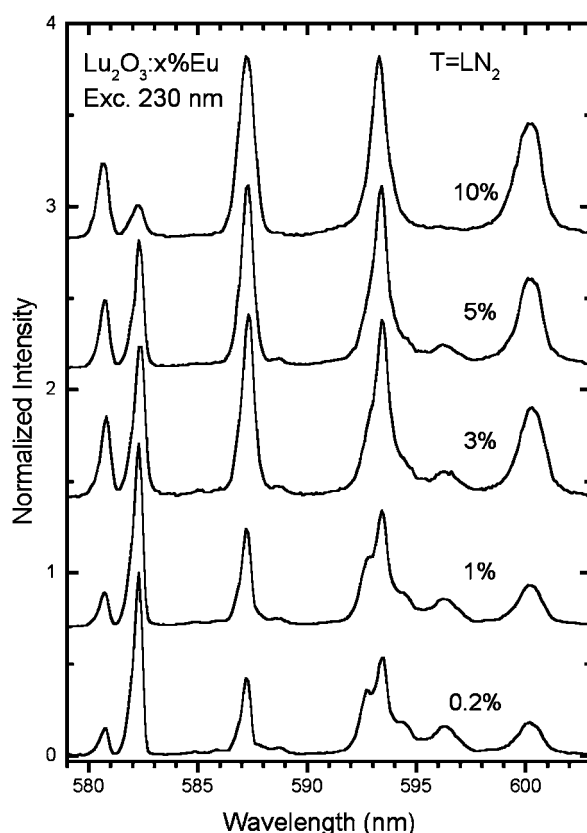


Figure 7. Concentration dependence of the emission of $\text{Lu}_2\text{O}_3:x\% \text{Eu}$ under a quasi-selective excitation into the $\text{Eu}(\text{S}_6)$ CT band at liquid nitrogen temperature.

(although not exclusively, see figure 4) excites the Eu ions located in the S_6 site. For clarity we present only the 580–605 nm emission range.

For the specimens of lower concentrations the 230 nm excitation favours the emission characteristic for $\text{Eu}(\text{S}_6)$. However, when the Eu content significantly increases we clearly see that the $\text{Eu}(\text{C}_2)$ luminescence intensity increases at the expense of the $\text{Eu}(\text{S}_6)$ one. This is exactly what would be expected, since with rising concentration of the activator the distance between the Eu ions decreases and the probability for energy exchange between them rises. We again see that the most probable energy transfer is the $\text{Eu}(\text{S}_6) \rightarrow \text{Eu}(\text{C}_2)$ one. We should note, however, that even for the relatively highly concentrated system, $\text{Lu}_2\text{O}_3:10\% \text{Eu}$, luminescence is still observed from the $\text{Eu}(\text{S}_6)$ ions. This may result either from the still available relatively isolated $\text{Eu}(\text{S}_6)$ ions or/and from the existence of a $\text{Eu}(\text{C}_2) \rightarrow \text{Eu}(\text{S}_6)$ back-transfer as we suspected earlier. The presence of such transfer was reported by Blasse [17] for $\text{Y}_2\text{O}_3:\text{Eu}$, which is the structural analogue of lutetia. Nevertheless, the emission spectra confirm that the main energy transfer process in the more concentrated systems is the $\text{Eu}(\text{S}_6) \rightarrow \text{Eu}(\text{C}_2)$ one, exactly as expected. Its rate at liquid nitrogen temperature becomes significant only for rather heavily doped samples, however. Therefore, for samples containing up to about 5% of the dopant the $\text{Eu}(\text{S}_6)$ emission (the lines around 582.8 nm and within 592–597 nm range) comprises a relatively significant part of the total luminescence. At liquid nitrogen temperature the Eu content must be as high as 10% to reduce the fraction of the $\text{Eu}(\text{S}_6)$ luminescence to

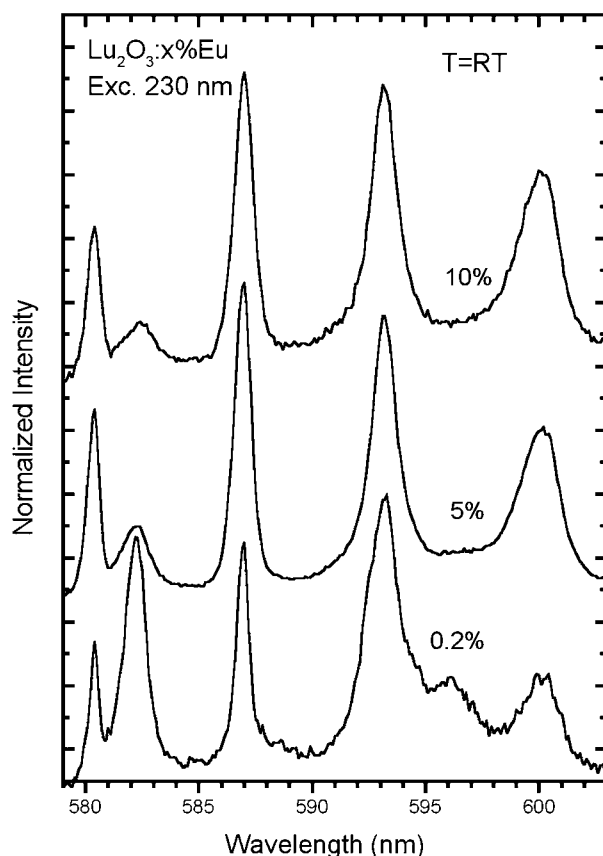


Figure 8. Concentration dependence of the emission of $\text{Lu}_2\text{O}_3:x\% \text{Eu}$ under a quasi-selective excitation into the $\text{Eu}(\text{S}_6)$ CT band at room temperature.

3.5% of the total of emitted light.

The situation changes when analogous processes are observed at room temperature. In figure 8 we present the concentration dependence of the emission from $\text{Lu}_2\text{O}_3:\text{Eu}$ within the region of 578–603 nm. For the most diluted specimen the $\text{Eu}(\text{S}_6)$ emission makes up a significant part of the total. However, comparing emissions from the 5 and 10% samples we do not see any difference in the ratio of intensities of the $\text{Eu}(\text{S}_6)$ (582.2 nm, $^5\text{D}_0 \rightarrow ^7\text{F}_1$) and $\text{Eu}(\text{C}_2)$ (580.2 nm, $^5\text{D}_0 \rightarrow ^7\text{F}_0$) lines. This means that already for the 5% specimen there was achieved an equilibrium between the $\text{Eu}(\text{S}_6) \rightarrow \text{Eu}(\text{C}_2)$ energy transfer and back-transfer processes. This further means that it is impossible to completely get rid of the $\text{Eu}(\text{S}_6)$ slower magnetic dipole luminescence from the $\text{Lu}_2\text{O}_3:\text{Eu}$. Nevertheless, its part in the total emission at room temperature can be diminished to <2% when the activator concentration reaches the level of about 5% or higher. This result does not practically change for different excitation energies, which means that at this point there exists a kind of equilibrium between the $\text{Eu}(\text{S}_6) \rightarrow \text{Eu}(\text{C}_2)$ energy transfer processes. Comparing results obtained at room temperature and at liquid nitrogen temperature we can state that the former facilitates the $\text{Eu}(\text{S}_6) \rightarrow \text{Eu}(\text{C}_2)$ energy transfer. This manifests in faster diminishing of the $\text{Eu}(\text{S}_6)$ emission lines with increasing dopant concentration and in stronger reduction of its fraction in the total emitted light at room temperature.

Let us note here that in the emission spectra we see two unexpected low intensity lines

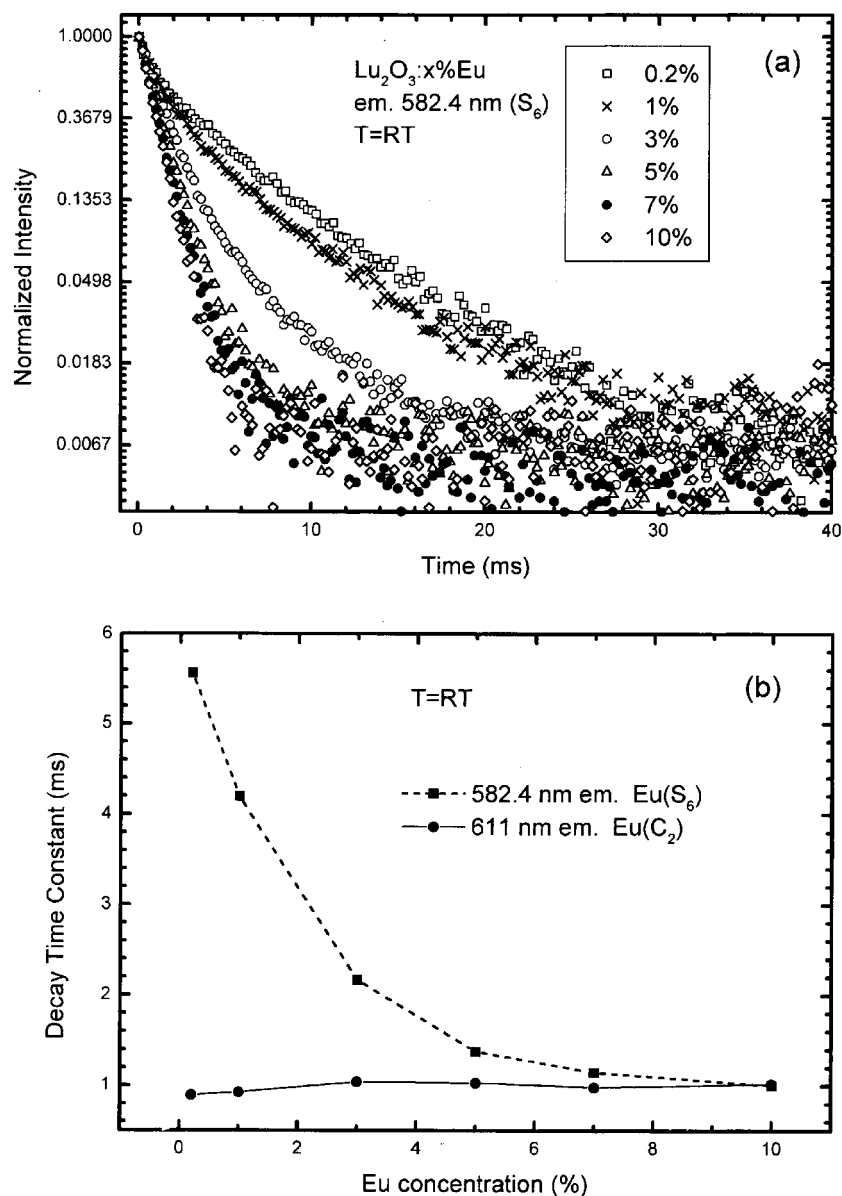


Figure 9. Room temperature concentration dependence of the 582.4 nm $\text{Eu}(\text{S}_6)$ luminescence decay kinetics (a) and concentration dependence of the time constants derived from the analytical fits to the decay traces of 582.4 nm $\text{Eu}(\text{S}_6)$ and 611 nm $\text{Eu}(\text{C}_2)$ emissions (b).

located around 594.6 nm and 596.5 nm. They accompany the $\text{Eu}(\text{S}_6)$ emission only. The same was observed in the case of Eu -doped Y_2O_3 and, lacking any better idea, the extra lines were assigned to vibronic transitions [19, 21]. Presently, we cannot offer any better explanation of origin of the lines in $\text{Lu}_2\text{O}_3:\text{Eu}$.

Both at liquid nitrogen temperature (figure 7) and at room temperature (figure 8) we can observe a systematic broadening of the luminescent lines with increasing dopant content.

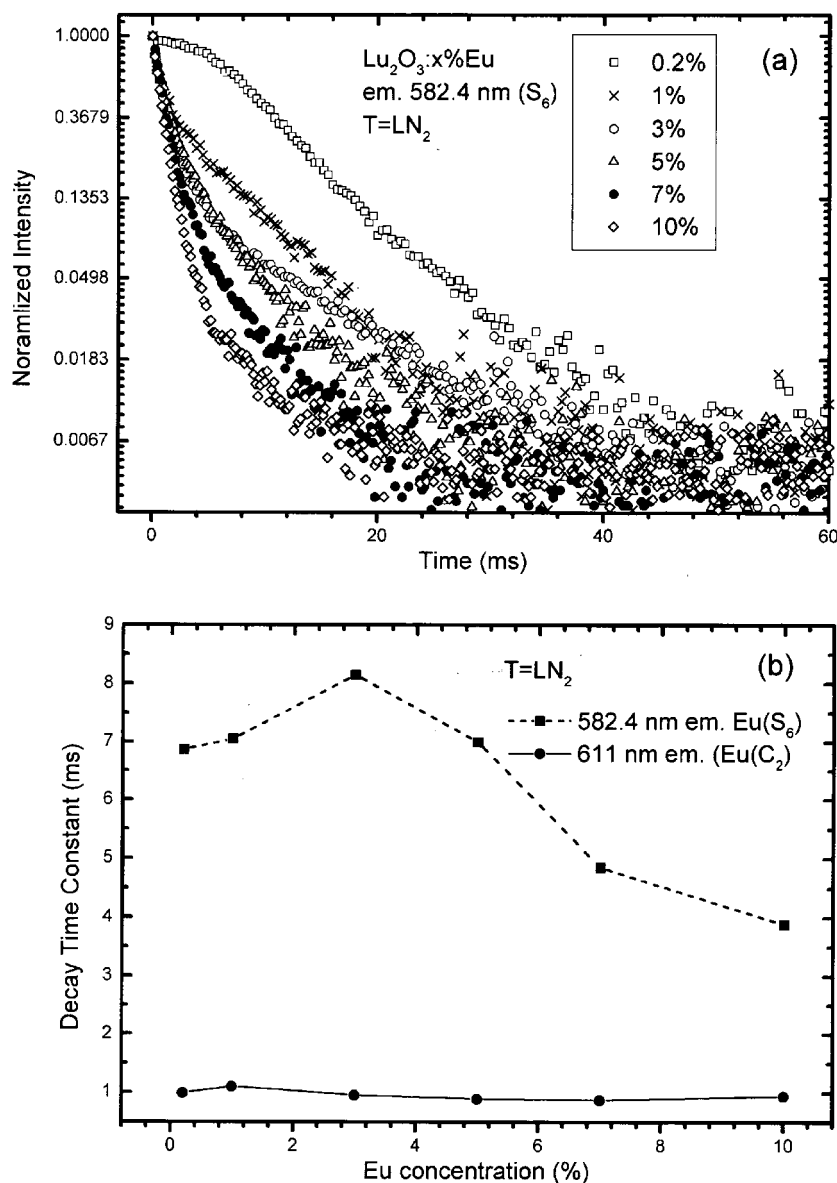


Figure 10. Liquid nitrogen temperature concentration dependence of the 582.4 nm $\text{Eu}(\text{S}_6)$ luminescence decay kinetics (a) and concentration dependence of the time constants derived from the analytical fits to the decay traces of 582.4 nm $\text{Eu}(\text{S}_6)$ and 611 nm $\text{Eu}(\text{C}_2)$ emissions (b).

This again confirms the existence of augmenting interactions between the activator ions with increasing concentration. Thanks to the Eu–Eu interaction we can significantly reduce the amount of light emitted by Eu ions occupying the S_6 site due to their ability to transfer their energy to the nearby located Eu ions residing in the C_2 site of the Lu_2O_3 host lattice.

The rising probability of the $\text{Eu}(\text{S}_6) \rightarrow \text{Eu}(\text{C}_2)$ energy transfer can be nicely observed through changes in decay kinetics of the specific emissions. Figures 9 and 10 present the results of such measurements at room and liquid nitrogen temperatures for the 582.4 nm emission of

$\text{Eu}(\text{S}_6)$ together with the changes in the time constants of the $\text{Eu}(\text{C}_2)$ and $\text{Eu}(\text{S}_6)$ emissions.

At both temperatures the general pattern is similar. The higher content of the dopant makes the $\text{Eu}(\text{S}_6)$ emission shorter. Rather surprisingly, the changes in the decay kinetics observed at room temperature are more straightforward than at liquid nitrogen temperature. At room temperature the decays could be fitted with two exponents independently of the concentration. For the most diluted specimen the main component reached 5.6 ms and was accompanied by a short constituent of about 1.0 ms. With rising concentration of the activator a still higher and higher portion of the emission was liberated with the short time constant of about 1.0 ms and the longer component systematically shortened. Finally, for the specimen containing 10% of the activator the decay became practically one-exponential with the time constant of 1.0 ms. Thus, indeed we see that the energy of excited ions of Eu^{3+} located at the S_6 site can be transferred into the $\text{Eu}(\text{C}_2)$ ions located nearby. This process becomes more and more efficient as the activator content increases. The room temperature results seem to indicate that by increasing the Eu concentration above 10% we could expect yet more profound quenching of the $\text{Eu}(\text{S}_6)$ luminescence. Let us note that the results are very similar to those presented by Forest and Ban for $\text{Y}_2\text{O}_3:\text{Eu}$ [16].

At liquid nitrogen temperature the behaviour of the materials (see figure 10) is generally similar to what was seen at room temperature. The decays could be reasonably fitted with two exponents. Nevertheless, the quenching of the $\text{Eu}(\text{S}_6)$ luminescence becomes profound only for higher concentrations at this lower temperature. As was seen at room temperature the long component is accompanied by a shorter one, whose time constant again reaches about 1.0–1.1 ms. The fraction of this constituent systematically increases with rising Eu concentration. Obviously, the presence of the short constituent in the decays of the $\text{Eu}(\text{S}_6)$ luminescence must necessarily result from quenching of this emission due to the $\text{Eu}(\text{S}_6) \rightarrow \text{Eu}(\text{C}_2)$ energy transfer. The higher the dopant content the more of the emission is being quenched and thus the larger part of the emission is characterized by the shorter time constant. We can yet see some, rather unexpected, variations in the time constant of the long component of the 582.4 nm emission of $\text{Eu}(\text{S}_6)$. Namely, it slightly lengthens up to the concentration of 3% and only above this level it becomes shorter dropping to about half of its initial value for the 10% specimen. The lengthening for the lower concentrations is not clear for us.

Let us state that neither at liquid nitrogen temperature nor at room temperature does the emission of Eu occupying the C_2 site exhibit any concentration dependence. Furthermore, the time constant of this emission is practically the same for both temperatures. Hence, we can state that the $\text{Eu}(\text{C}_2)$ emission does not show any signs of concentration or temperature quenching up to 10% of the Eu concentration.

In the $\text{Eu}(\text{S}_6)$ emission decay kinetics of the 0.2% specimen measured at liquid nitrogen temperature a rise of the signal characterized by a time constant about 1.3 ms is clearly seen, close to the decay time of the $\text{Eu}(\text{C}_2)$ luminescence. The effect is not observed for any other concentrations investigated. While presently we cannot offer any reliable explanation of these effects we wish to note that the closeness of the $\text{Eu}(\text{S}_6)$ rise time (for 0.2% sample) to the radiative life time of the $\text{Eu}(\text{C}_2)$ emission does not have to be accidental. This may have something to do, for example, with a $\text{Eu}(\text{C}_2) \rightarrow \text{Eu}(\text{S}_6)$ back transfer.

The results of decay kinetics measurements clearly confirm the existence of the $\text{Eu}(\text{S}_6) \rightarrow \text{Eu}(\text{C}_2)$ energy transfer and prove that the transfer is strongly temperature dependent, becoming more efficient at higher temperatures. The analysis of the decay kinetics generally confirms the conclusions we drew discussing luminescence spectra presented in figures 7 and 8. Furthermore, we note that for concentrated systems at room temperature the slow magnetic dipole emission of $\text{Eu}(\text{S}_6)$ can be significantly quenched and its time constant can be reduced to the value characteristic for the faster electric dipole luminescence of $\text{Eu}(\text{C}_2)$ — ~ 1.0 ms.

4. Conclusions

Our relatively simple spectroscopic measurements confirmed that Eu ions enter both available symmetry sites in the lutetia host lattice. We showed that both the f-f and CT levels of the Eu(S₆) sites are situated slightly above those of the Eu(C₂) site. We proved that with increasing activator concentrations the rate of energy transfer between the Eu ions located in the two sites also increases and the rate of the Eu(S₆) → Eu(C₂) energy transfer significantly surpasses the opposite-direction back-transfer. Nevertheless, even selective excitation of the Eu(C₂) ions creates some of the Eu(S₆) emission, which indicates the presence of the Eu(C₂) → Eu(S₆) back-transfer, too. Therefore, it is not possible to completely get rid of the slower Eu(S₆) luminescence. Nevertheless, the efficient Eu(S₆) → Eu(C₂) energy transfer for higher concentrations reduces the fraction of the Eu(S₆) emission to a reasonably low quantity of 2–3.5% of the total, depending on the temperature. At room temperature, for higher Eu concentrations the time constant of the Eu(S₆) luminescence drops to the value characteristic for the Eu(C₂) luminescence (~1.0 ms). The relative positions of the Stark levels of Eu³⁺ in Lu₂O₃ were shown to be very similar to those found in Y₂O₃ by other authors.

Acknowledgments

The author thanks Mrs J Trojan for technical assistance and Dr Hreniak for measurements of decay kinetics. We also gratefully acknowledge the funding of this project by the Polish Committee for Scientific Research (KBN) under grant No 3 T09B 031 16, and by NATO under grant No PST.CLG.976212.

References

- [1] Laversenne L, Guyot Y, Goutaudier C, Cohen-Adad M Th and Boulon G 2001 *Opt. Mater.* **16** 475–83
- [2] Brenier A and Boulon G 2001 *J. Alloys Compounds* **323/324** 210–13
- [3] Garcia-Murillo A, Le Luyer C, Pedrini C and Mugnier J 2001 *J. Alloys Compounds* **323/324** 74–7
- [4] Weber M J, Derez S E, Dujardin C and Moses W W 1996 *Proc. Scint'95 (Delft)* ed P Dorenbos and C W E van Eijk, pp 9–16
- [5] Derez S E, Moses W W and Cahoon J L 1991 *IEEE Nuclear Science Symp. Conf. Record* 91CH3100-5, vol 1, pp 143–7
- [6] Zych E, Dereń P J, Stręk W, Meijerink A, Domagała K and Mielcarek W 2001 *SPIE* **4413** 176–81
- [7] Zych E, Dereń P J, Stręk W, Meijerink A, Mielcarek W and Domagała K 2001 *J. Alloys Compounds* **323/324** 8–12
- [8] Zych E 2001 *Opt. Mater.* **16** 445–52
- [9] Derez S E, Moses W W, Weber M J and West Z C 1994 *Mater. Res. Soc. Symp. Proc.* **348** 39–49
- [10] Blasse G and Grabmeier B C 1994 *Luminescent Materials* (Berlin: Springer)
- [11] FIZ Karlsruhe & Gmelin Inst. 1990 *ICSD Collection* 40471, release 99/1
- [12] FIZ Karlsruhe & Gmelin Inst. 1990 *ICSD Collection* 86815, release 99/1
- [13] Saiki A, Ishizawa N, Mizutani N and Kato M 1984 *Acta Crystallogr. B* **40** 76–82
- [14] Baldinozzi G, Berar J-F and Calvarin G 1998 *Mater. Sci. Forum* **278** 680–5
- [15] Shannon R D 1976 *Acta Crystallogr. A* **32** 751–67
- [16] Forest H and Ban G 1969 *J. Electrochem. Soc.* **116** 474–778
- [17] Buijs M, Meijerink A and Blasse G 1987 *J. Lumin.* **37** 9–20
- [18] Dieke G H 1968 *Spectra and Energy Levels of Rare Earth Ions in Crystals* (New York: Wiley-Interscience)
- [19] Leavitt R P, Gruber J B, Chang N C and Morrison C A 1982 *J. Chem. Phys.* **76** 4775–88
- [20] Gruber J B, Leavitt R P, Morrison C A and Chang N C 1985 *J. Chem. Phys.* **82** 5373–8
- [21] Pappalardo R G and Hunt R B Jr 1985 *J. Electrochem. Soc. Solid State Sci. Technol.* **132** 721–30
- [22] Zych E, Karbowski M, Domagała K and Hubert S *J. Alloys Compounds* at press